APPLICATIONS OF THE DYNAMICAL AND STATISTICAL DOWNSCALING TECHNIQUES TO THE LOCAL MULTI-DECADE WAVE SIMULATIONS

Lidia Gaslikova

GKSS Research Center, Institute for Coastal Research
Max-Planck Str. 1, 21502 Geesthacht, Germany
e-mail: lidia.gaslikova@gkss.de

1 INTRODUCTION

Many applications in coastal engineering require knowledge about extreme wave statistics at or near the coastal facilities. The data for such statistics are often limited or sometimes even nonexistent. Measurements from a nearby location are frequently used instead. In combination with more or less sophisticated methods to transfer the information to the place of interest, measurements are used to derive the relevant statistics (e.g., Coastal Engineering Manual, Eurowaves project, JERICHO project). When such measurements are not available or lack homogeneity that prevents the estimation of reliable statistics, multidecadal wave hindcasts may be an alternative. In recent years, multidecadal simulations of ocean waves have become more and more common (e.g., WASA Group 1998; Günther et al. 1998; Cox and Swail 2001; Weisse et al. 2002; Caires et al. 2002; Sterl et al. 1998; Kushnir 1997). Most of these studies have been motivated by concerns about possible ongoing long-term changes in the wave climate (especially in the extreme sea states) and their consequences for coastal protection and the safety of humans living at the coast. While large-scale changes may be reasonably estimated from these simulations, their value for the design and safety assessment of coastal protection structures may be limited due to their relatively coarse spatial and temporal resolutions. Another reason for this is that shallow water effects are usually not accounted for in most of these simulations. In addition, because of computational constraints their spatial resolution remains limited and may be too coarse to be used directly for coastal design purposes. For the latter, additional techniques are required to transfer the wave information from such a hindcast to the site of the construction.

The main objective of the present study is to select or develop downscaling method appropriate for the localization of the existing regional wave data for several decades. The surroundings of the Helgoland Island were chosen as the test and application area. Local wave effects are expected in the region because of the presence of two islands of rather small size (about 1 km^2) and complicated bathymetry in the surrounding area. This also allows the testing of the quality of the regional hindcast in an environment for which it was not explicitly intended. The first proposed downscaling method is the dynamical wave modeling. Until now most of the high-resolution dynamical wave-modeling experiments have been made for episodical wave simulations of selected storms or case studies and the modeled time period of such simulations varied from several hours to several years (e.g. Vierfuss 2002). Here the ability of the dynamical models to produce multi-decade wave simulations and provide adequate wave statistics is investigated and discussed. The statistical downscaling models applied to the medium-scale wave data could provide an alternative to dynamical wave modeling. The statistical downscaling experiments for the ocean waves were earlier limited by the applications to the downscaling of extreme wave statistics on the coarse (tens of kilometers) spatial scale (e.g. Kushnir et al. 1997, WASA Group 1998, Wang and Swail 2001). In this study the statistical models were applied to the localization of instantaneous wave fields and high-resolution coastal wave applications.

The paper is structured as follows: In Section 2 the dynamical wave model is described; the results of the modeling are compared with observations. The medium and small-scale wave data are compared with the goal of evaluating the added value obtained by the high-resolution modeling. The statistical-dynamical approach is described in Section 3. Three statistical methods are applied to the localization of the regional wave data. The results are compared between each other and with the outcome from the dynamical model. The local wave climate for Helgoland for the last four decades obtained with the statistical model is presented and discussed in the Section 4. Summary and some additional remarks conclude the paper.

2 DYNAMICAL MODELING

2.1 METHODS AND EXPERIMENTS

The reference regional wave data were obtained from the multi-decade wave hindcast 1958–2002 for the Southern North Sea provided by Weisse et al. (2002). The simulation has been produced within the HIPOCAS (Hindcast of Dynamic Processes of the Ocean and Coastal Areas of Europe) project (Soares et al. 2002). This dataset represents the longest homogeneous wave hindcast available at the presently unsurpassed spatial resolution of about 5.5 km and also takes into account shallow water effects. The wave fields were modeled with the WAM model (WAMDI Group 1988). Several runs with different spatial resolutions were produced within the project. Here the finest run with a resolution of 5×5 km covered the North Sea south from 56°N is used (referred as HF run). It was driven by hourly wind fields at 50 km resolution obtained from an atmospheric hindcast performed with the REMO model (Feser et al. 2001). For HF hindcast water level variations were also taken into account. Hourly water level and current components were provided by BAW (Coastal Division of the Federal Waterways Engineering and Research Institute). They were obtained on an irregular grid (about 200 m for the German Bight) using the storm–surge model TELEMAC-2D (A. Pluess, 2003, personal communication).

For the dynamical downscaling of the reference data (HF), the K-model (Schneggenburger et al. 1997) was adopted. The K-model represents a third generation shallow water wave model that captures features of the large-scale forcing and adds to them the small-scale effects not resolved by the driving large-scale data. It is a discrete spectral wave model solving the wave action balance equation in the wave number domain. A modified Philips linear function (Cavaleri and Rizzoli 1981) and a modified Snyder exponential function (WAMDI Group 1988) parameterize energy input by the wind. Nonlinear wave–wave interactions have been neglected following the reason of Schneggenburger (1998) who argued that in shallow water the assumptions of homogeneity for the application of this theory are violated. Instead, a nonlinear dissipation source function (Günther and Rosenthal 1995; Schneggenburger et al. 1997) accounting for the dissipation by wave turbulence is used. Bottom dissipation is taken into account according to Hasselmann et al. (1973). In addition, refractions caused by currents and depth are also included. The tunable parameters were set up according to Schneggenburger (1998) set for the limited fetch growth. A comparison of the model performance relative to other shallow water wave models is presented in Moghimi et al. (2005).

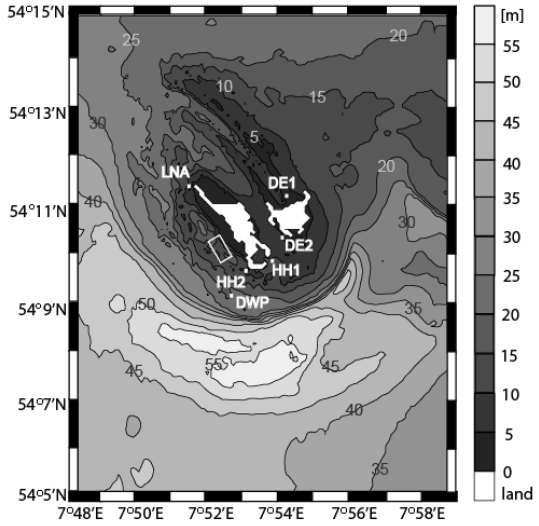

Fig. 1 K-model domain and bathymetry in meters. The location of a deepwater buoy used for validation is indicated by DWP. The rectangle indicates the area for which radar measurements taken from a telecommunications tower at the main island are representative. LNA, HH1, HH2, DE1, and DE2 represent model points near coastal facilities and are used for assessing model performance

The model was set up for the vicinity of Helgoland, an island located in the German Bight (Fig. 1). The model domain comprises an area of about 15×15 km at a spatial resolution of 100×100 m. The bathymetry was obtained from the BAW (N. Winkel, personal communication) with a resolution of about 50 m on an unstructured grid and was interpolated to the K-model resolution. A propagation time step of 4 s was adopted. Forcing sources comprise hourly near-surface wind fields, water level, and current fields obtained from the HIPOCAS hindcasts and have been interpolated to K-model grid. As boundary conditions, 3-hourly wave spectra from HF reference run were used. The K-model was integrated for the 12-year period 1990–2001. The results of this simulation have been stored hourly in the form of integrated wave parameters such as significant wave height (SWH), peak period, peak wave direction etc. at all grid points and as two-dimensional wave spectra at selected model grid points (see Fig. 1). In this set-up, the Kmodel simulation can be considered as a dynamical downscaling of the HIPOCAS wave hindcast. In the following, this simulation will be referred to as the K-model hindcast (KMH).

2.2 VALIDATION OF K-MODEL RESULTS

For the period of interest there were no long-term measurements close to coastal facilities

but within the model area two observed wave datasets are available. The first one is provided by the BSH (Bundesamt für Seeschiffahrt und Hydrographie) waverider buoy located approximately one kilometer south-west from the island. The water depth there is about 20 m. The measured quantities comprise 9 parameters from which significant wave height, peak period and mean direction for the period from March 1998 to October 2001 are used for the comparison with the K-model results. Another data source is the WaMoS II (Wave and Surface Current Monitoring System) radar (Hessner et al. 2001) permanently mounted on a telecommunication tower on the main island since March 1998 and providing wave parameters averaged over the rectangular surface area in a distance of about 500 m south-west from the islands (Fig. 1).

At first, to assess the quality of modeled instantaneous values with respect to observations, significant wave heights, peak periods and mean directions from all three data sources (K-model, buoy and radar) were compared for October 1998 (Fig. 2) and in general a good agreement between all datasets can be inferred. A closer look at differences provides a reasonable explanation for the major part of them. At the first decade of examined month the modeled SWH values are lower at the radar area than at the buoy position. At the same time easterly wind dominates the territory which causes the island shadow effect in the area located west from the islands making the waves smaller. This effect is diminished at the DWP position located farther to the south, which is in agreement with the buoy observations (Fig. 2, upper panel). The radar data for this case is not available. For the second part of the period considered, the buoy and the radar observations are close to each other as well as to the model results at the two locations. The discrepancy between observed and modeled data occurs for some high wave situations where SWH appears to be overestimated by the model. The impact of the boundary conditions (HF) on the K-model results is discussed later. For peak periods, more pronounced differences between buoy and radar locations for the measured as well as for modeled data can be detected. Slight overestimation of peak periods by the model, especially for some high wave situations, can be observed. The measured wave directions are similar for both locations and the hindcast produced by the K-model appears to be quite reasonable and close to the observations.

Figure 3a shows a comparison of modeled and observed significant wave height distribution for the period 1998-2001. For the lower 90% of the distribution a rather good agreement between model and buoy observations can be seen. In the

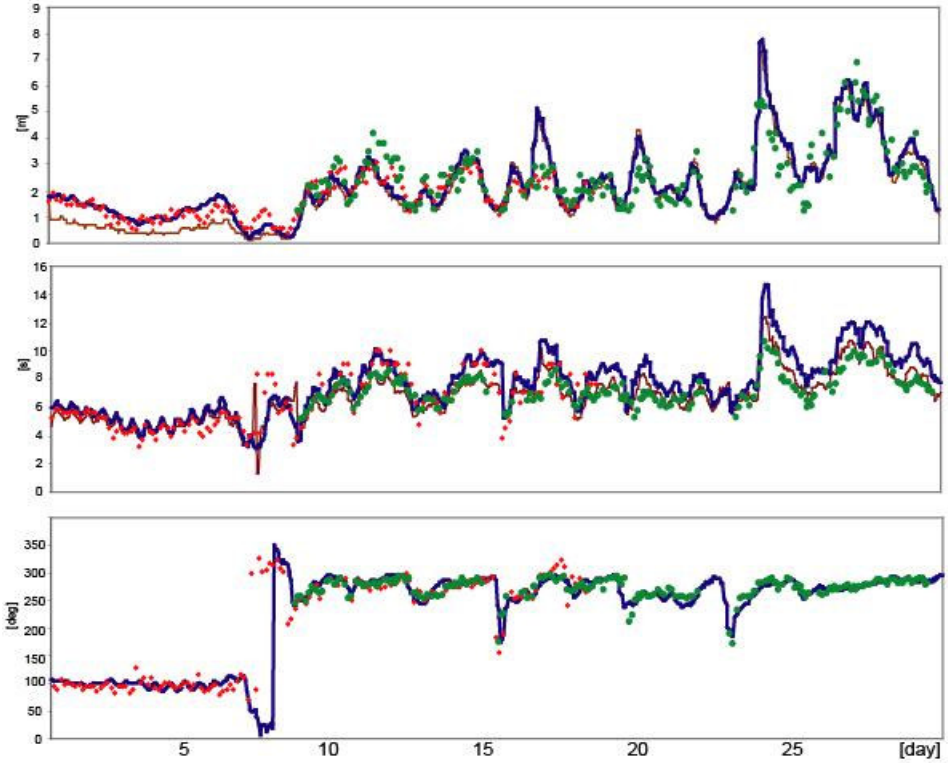

Fig.2 Hindcast (KMH) and observed wave parameters at DWP and the central point from the area covered by radar measurements for October 1998. From top to bottom: significant wave height in meters, peak period in seconds and mean direction (coming from) in degrees. Buoy measurements are shown as crosses, radar measurements are shown as circles. The K-model hindcast at the buoy (DWP) location is given by a blue line; hindcast at the central point of radar rectangular is given by a brown line.

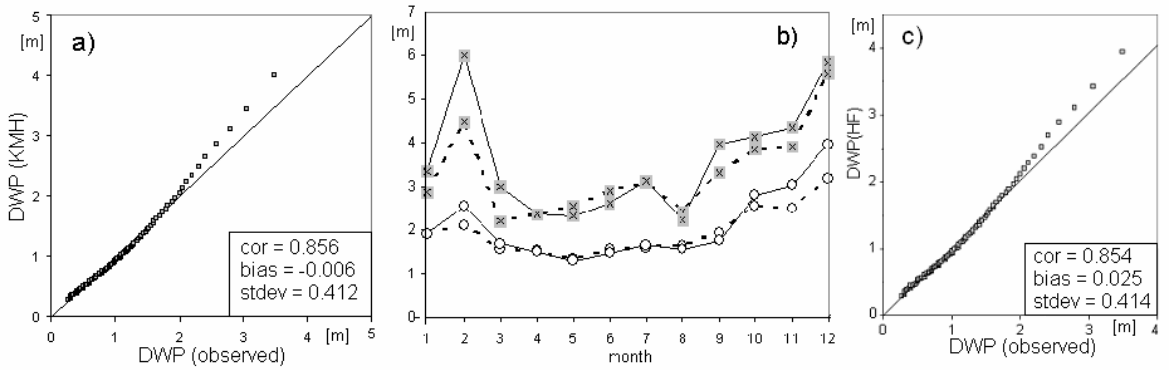

Fig.3 a) Quantile-quantile plot of observed by buoy (x-axis) and hindcast by K-model (y- axis) significant wave heights at DWP for 1998-2001. Quantiles from 0.05 to 0.99 are shown with 0.01 interval. b) Observed (dashed) and hindcast (*solid*) monthly 90%-tiles (*circles*) and 99%-tiles (*crosses*) of significant wave height at DWP. In all cases quantiles have been compared only for dates for which observational data have been available. c) Quantile-quantile plot of observed by buoy (x-axis) and hindcast by HIPOCAS (y-axis) significant wave heights at DWP for 1998-2001. Quantiles from 0.05 to 0.99 are shown.

range between about 1.0 to 1.5 meters the K-model slightly underestimates the buoy data. For the highest 10% of the waves an overestimation by the K-model of up to 80 cm can be inferred, indicating that the highest waves occur too often or are too severe in the KMH simulation. Figure 3b shows a more detailed comparison of observed and hindcast averaged monthly 90-th and 99-th percentiles. For the 90-th percentile a reasonable agreement can be inferred. An exception is found in the months November, December and February for which the model tends to show higher extremes. A similar condition holds for the 99-th percentile that represents the most extreme events. For the 99-th percentile KMH values are somewhat higher also for March, September and October.

To check whether the overestimation of the high waves is caused mainly by the driving boundary conditions or by the K-model physics, percentiles of the HF hindcast and the buoy SWH data were compared (Fig. 3c). The overestimation of observed high waves was found to be of the same order of magnitude for the HF run as for the K-model. This bias in upper percentiles of boundary conditions (HF) is consistent with the results of the HF comparison with satellite data for the German Bight (not shown, see e.g. Gaslikova 2006). This behaviour can be explained by deficiencies of the model spatial resolution or by the uncertainties in driving forcing and model physics of the HF run. In case the bias is caused by a too coarse spatial resolution of the HF run, the K-model is supposed to improve the wave data representation with respect to HF by taking into account processes on finer scales. However, this can be not the case for the buoy position because of the relatively deep water at the location (20 m), which diminishes the importance of such wave processes as refraction and bottom dissipation. The errors in the HF data caused by uncertain external forcing or internal physics can hardly be corrected by the K-model because a higher (in case of overestimation) energy is expected to be transferred by the K-model to the interior locations from the boundaries. Consequently, it can be concluded that the overestimation of the most severe wave events is at least partially a result of the too high waves provided at the K-model boundaries. In addition to the biased boundary conditions, the possible reasons of the K-model and buoy data discrepancies are the uncertainties in bathymetry and wind data used by the K-model as well as measurement errors.

2.3 ADDED VALUE FROM THE SMALL-SCALE WAVE SIMULATION

The previous section demonstrated the similarity of the local wave parameters modeled by the K-model and measured wave data. The differences between the model results and observations at DWP can mainly be attributed to the driving HF hindcast. Based on this, it is assumed that the small scale features simulated by the K-model share some resemblance with reality and, therefore, the KMH experiment is considered in the following as a substitute for reality. This allows the testing of to what extent improvements in the representation of near shore extreme wave statistics can be achieved by the application of dynamical wave modeling (here K-model) to the medium-scale wave data (here HF). The improvement will be assessed relative to the HF hindcast, as these data is readily available and thus can be considered as a first guess of the prevailing near-shore wave conditions.

First the extent to which the HF hindcast may be used to reasonably assess long-term wave statistics in the coastal zone is investigated. Here the evaluation is mainly focused on the statistics of extreme events for the significant wave heights as they are essential for coastal protection. Two datasets are analyzed, namely significant wave height from the HIPOCAS fine grid hindcast with

about 5 km resolution (HF) and the KMH hindcast with 100 m resolution driven by the HF run (see also Fig. 1).

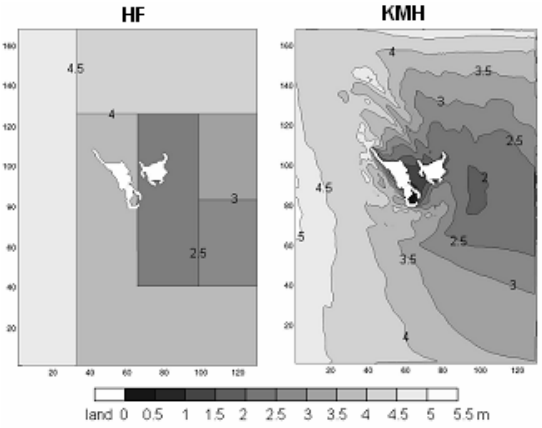

Fig. 4 Ninety-nine percentile of significant wave height in meters derived from 3-hourly values for the period 1990–2001 from the HF hindcast (*left*) and KMH experiment (*right*)

Figure 4 shows a comparison between the 99-th percentiles of significant wave height for the period 1990-2001 obtained from the HF and the K-model hindcast. It can be seen that for both simulations a similar large-scale pattern of extreme wave statistics is reproduced. The pattern is characterized by highest waves occurring in the western part of the K-model domain that continuously decrease eastwards. East of Helgoland a distinct area with relatively low wave extremes can be found which is mainly caused by the shadowing effect of the islands against the prevailing wind and wave directions. The large-scale similarity between both simulations is primarily a consequence of both simulations having identical wave conditions at the K-model boundaries or, in other words, that the K-model uses boundary conditions from the HF hindcast. In addition, the same wind fields have been used in both simulations.

Despite a large-scale similarity between the HF and the KMH hindcasts, small scale differences in extreme wave statistics are obvious (Fig. 4). In particular, the island shadow effects are more pronounced and extend further eastward in the K-model simulation. South-eastwards of Helgoland the 99-th percentile of significant wave height is about one meter higher compared to the HF simulation. Furthermore, for the K-model run, small scale features of the bathymetry are visible in the distribution of the wave extremes. While large-scale features of extreme wave statistics are quite similar in both simulations, the small scale differences may be significant for coastal protection. Figure 5 shows a comparison of the frequency distribution for significant wave heights near different coastal facilities obtained from the HF and the KMH hindcasts. The positions of the analyzed points can be inferred from Figure 1. Although the K-model is driven with boundary conditions from the HF run and both simulations utilize the same wind forcing, differences in the frequency distributions, in particular for near coastal locations, do emerge. The details of these differences depend on the location. At DWP both hindcasts are rather similar. Here water depth is about 20 meters and the shadowing effect of the island plays a minor role as the prevailing wind and wave directions are from the southwest to the northwest. At LNA the situation is different. LNA is also located at the western side of the island, but here bathymetry effects become important. While

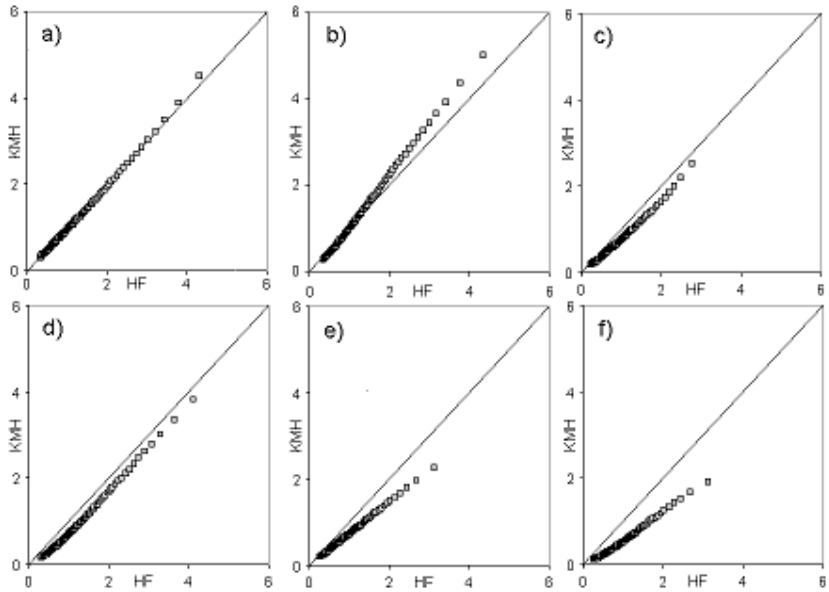

Fig.5 Quantile-quantile plots of HF and KMH simulated significant wave height in meters for the period 1990-2001 at points a) DWP b) LNA c) HH1 d) HH2 e) DE1 f) DE2

the lower 75% of the simulated wave height distributions are still rather similar in the HF and the KMH, the uppermost 20% are remarkably higher in the K-model simulation (Fig. 5b), demonstrating the results of shoaling for the KMH waves. Near the Helgoland harbor (HH1, HH2) shallow water effects and the strong gradients in the bathymetry play a significant role. Here small water depths cause the reduction of the wave heights and, independently of their heights, waves are generally lower in KMH. To the east of the main island, waves are also generally smaller in the K-model hindcast. This can be inferred from the comparison of the wave height frequency distributions at DE1 and DE2, two locations near the coastal protection structures at the north and south shores of the smaller Düne Island (Fig. 5e,f). Generally, the effect is larger for higher waves and mainly results from a combination of lee and shallow water effects. Although the differences between HF and KMH wave statistics are significant and strongly location dependent, it appears, that for all locations the relationship between KMH and HF wave statistics is almost linear which is also the case for the instantaneous SWH values (not shown).

3. STATISTICAL-DYNAMICAL MODELING

3.1 METHODS

It has been shown in the previous section that for an adequate assessment of the near-shore wave statistics the large-scale wave data needs additional processing or downscaling. The spectral wave model provides successful dynamical downscaling. However, faster methods are sometimes required, especially in case of long-term hindcasts or scenario studies and of limited computational resources. The strong dependency of the local (KMH) wave parameters on the boundary conditions (HF) provides the opportunity to apply less time-consuming statistical downscaling models transforming medium-scale HF wave conditions directly to the detailed high-resolution wave fields. To test the extent to which statistical downscaling in combination with high-resolution dynamical wave modeling can be used to assess the near-shore wave climate, several statistical methods are applied to the problem. The basis for the construction of the statistical inter-scale relationships is provided by medium-scale wave fields obtained from the HF hindcast and the local wave data from the K-model simulation. The methods chosen for the experiment are linear regression, Canonical Correlation Analysis (CCA) and analogs (e.g. von Storch and Zwiers, 1999). Downscaling techniques such as CCA or analogs are often applied to monthly, seasonal or annual statistics (e.g. Zorita and von Storch 1999 or WASA Group 1998). However, some applications, such as the simulation of ship movements, would require high-resolution instantaneous data. Therefore, the extended downscaling concept is proposed and its ability to estimate 3-hourly wave data is tested. Instead of directly linking large and small scale wave statistics, all statistical models related 3-hourly wave data from the HF and the K-model hindcast. Small-scale wave statistics is derived subsequently from the instantaneous data. In the case of reliable and sufficiently homogeneous long-term measurements being available at the site of the construction, these may be used instead of the K-model data. However, when such data are not available or if information is required also for some surrounding area, a very high-resolution wave model simulation (such as KMH) validated with at least some existing data will represent the best possible option.

The K-model hindcast period was split into a 5-year fitting period (1990–1994) and a 7-year validation period (1995–2001) to fit and test the statistical models. For linear regression (LR), 3-hourly SWH and wind direction from a single grid point in the HF simulation located near the southwestern boundary of the K-model domain have been chosen as predictors. The regression model is conditioned upon the wind directions such that eight different regression models are built depending on wind coming from the 45-degree eight sectors starting from [−22.5, 22.5]. For each grid point *i* in the K-model domain and each of the eight-wind direction sectors *j*, a regression model

$$y_{i,t} = a_{i,j} x_t + b_{i,j} \qquad (1)$$

was built, where $y_{i,t}$ represents downscaled wave height, and x_t represents the predictor (HF wave height) . The coefficients $a_{i,j}$ and $b_{i,j}$ were fitted using a least-square method.

For both CCA and Analog methods the medium-scale HF 3-hourly significant wave height at the locations around the islands were used as predictors. The local KMH 3-hourly significant wave height were used as predictand. For the CCA the number of degrees of freedom was reduced by applying the empirical orthogonal functions (EOF) (e.g. von Storch and Zwiers 1999), which have been computed for the HF and the KMH SWH anomaly fields. For the HF dataset the leading two EOFs explain about 99.1% of the total SWH anomaly variance, for the K-model dataset the explained variance is about 98.3%. CCA patterns were computed subsequently based on the two leading EOFs, and SWHs for the validation period have been derived on the basis of those patterns.

For the analog method a pool of analogs

Table 1 Bias and standard deviation of errors in meters between significant wave heights obtained from KMH and different downscaling techniques for the points near coastal facilities

STDEV(error) [m]	DWP	LNA	HH1	HH2	DE1	DE2
KMH – HF	0.159	0.302	0.191	0.286	0.272	0.289
KMH – LR	**0.097**	**0.163**	**0.104**	**0.159**	**0.128**	**0.085**
KMH – CCA	0.108	0.255	0.179	0.19	0.163	0.13
KMH - Analog	0.224	0.364	0.234	0.385	0.218	0.184
BIAS [m]						
KMH – HF	-0.04	0.045	-0.17	-0.257	-0.228	-0.39
KMH – LR	**-0.004**	**-0.011**	**0.0002**	**-0.0008**	**-0.019**	**0.0006**
KMH – CCA	-0.005	-0.023	0.015	-0.004	-0.025	0.009
KMH - Analog	-0.012	-0.022	0.007	-0.012	-0.2	0.004

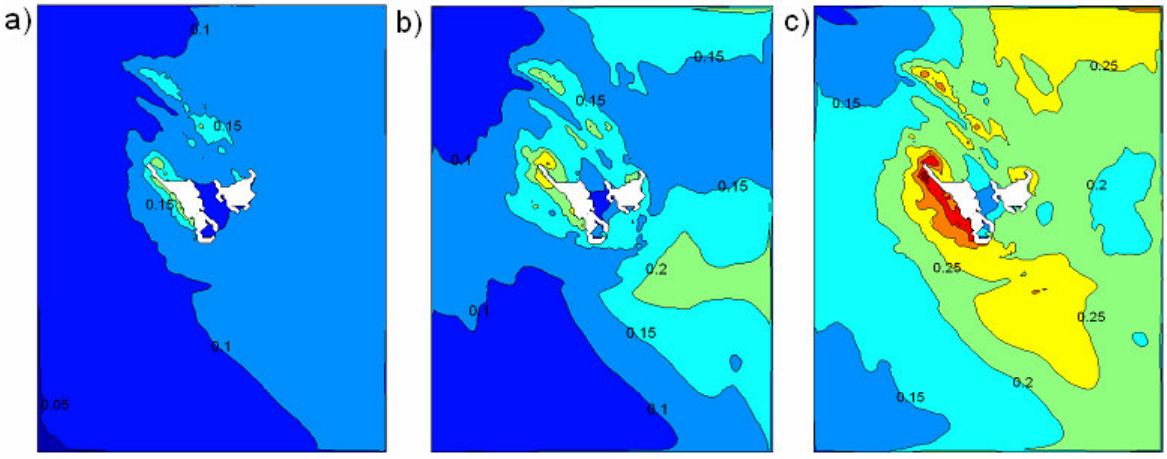

Fig. 6 Root mean square errors between instantaneous significant wave heights obtained from statistical methods a) LR, b) CCA, c) analog and KMH in meters

was constructed from the 3-hourly SWH fields 1990-1994 of the KMH hindcast and the corresponding principal components of the leading two EOFs of the 3-hourly HF SWH anomaly field. Subsequently an analog for each date of the validation period was determined. For this, the HF SWH data of the validation period was projected onto the first two EOFs for the fitting period and for each pair of principal components obtained the nearest pair (analog) from the training period was determined. The KMH wave height field belonging to this pair was then selected as the analog wave height field for the corresponding date in the validation period.

3.2 COMPARISON OF THE RESULTS

To test the skill of different downscaling methods in representing near-shore wave climate and, in particular, the instantaneous significant wave height, results obtained using different techniques have been compared with those from the KMH simulation. Table 1 shows the bias and the standard deviation of the SWH difference at the various locations specified in Figure 1 for the different downscaling models. It can be seen that the bias is largest when coarse grid data from the HF simulation are used directly to estimate the wave conditions at the near-shore locations. The largest standard deviations of SWH differences occur for the HF and analog data depending on the location. So, it appears that the SWH data produced with the analog method differs from KMH with the variance rate similar to HF but with much less bias than the medium-scale data. For linear regression and CCA the results are comparable. LR provides slightly smaller error with standard deviation up to 0.17 m and bias less that 0.02 m depending on the location.

The degree of difference between KMH and statistically obtained instantaneous SWH fields for the entire model area is assessed by the root mean square error (rms). The spatial patterns of the differences between KMH and each of three models are shown in Figure 6. The rms values vary between 0.05 and 0.2 meters for linear methods (LR and CCA) and reach up to 0.4 meters for the analogs. Although the spatial patterns and magnitudes differ, there are several regularities valid for all methods. So, for the western and

south-western parts of the modeled area the minimum errors over the entire domain can be seen, which means that the skill of the constructed models in representation of the wave heights at these locations is the best. The shape of this better represented area is similar to the contour-lines of the bathymetry and corresponds to the relatively deep water area. Further to the east the depth becomes less than 20-25 meters and the increasing error values can be observed. For all methods the maximum differences with respect to the dynamically obtained wave heights occur along the north-western Helgoland coast. Here the steep depth gradient causes intensive bottom dissipation and shoaling. These processes are sensitive to the variable water depth and the SWHs here are only partially dependent on the boundary conditions and approaching external waves. Therefore, the statistical models are not able to provide equally accurate wave reconstruction as for the deep water areas. Similar considerations apply to the area to the north from the island where the oblong shoal activates the shallow water processes, which makes the accurate SWH representation not completely feasible for the statistical methods.

Now the ability of different downscaling techniques in representation of extreme wave statistics for the entire model domain is assessed. For that the annual 99-th percentiles of SWH at each grid point for the validation period 1995-2001 are compared. The skill of the methods to improve the regional SWH representation is measured using the Brier skill score (B) (von Storch and Zwiers 1999).

$$B = 1 - S_{for}^2 / S_{ref}^2 \qquad (2)$$

Here S_{for}^2 and S_{ref}^2 represent the mean squared errors of the "forecast" (in this case provided by different downscaled data sets LR, CCA and Analog) and "reference forecast" (here HF hindcast) with respect to observed data. In face of missing observations the K-model simulation represents the substitute reality. Any positive value of B indicates that the downscaling method achieves an improvement relative to the HF data. The best performance corresponds with B=1, which means that the downscaled data is as good as the "observations". A negative value of B indicates that the method performs worse than the HF reference. The result is shown in Figure 7. As it can be seen, all statistical methods introduce enormous additional skill in representation of the spatial distribution of the SWH annual 99-th percentile relative to using data from the HF hindcast directly. Depending on the method the skill varies from 0.9 to 0.99 except for the analog method in the year 2001, where the skill score fell down to the 0.81. The linear regression shows the best and the least variable skill score values higher than 0.95 independently of a year. The analogs shows the worst performance in wave extremes representation which is consistent with the results for the instantaneous values comparisons. Nevertheless, the improvement obtained with all techniques is significant.

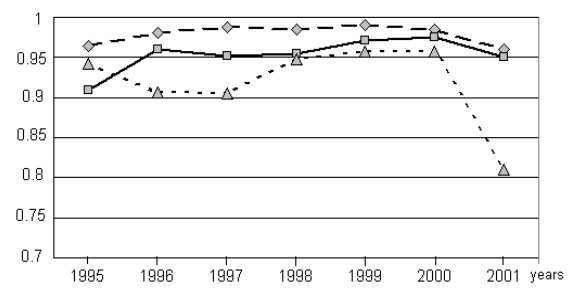

Fig. 7 Brier scores for the 99%-tile of yearly significant wave heights from 3 statistical methods: LR (*dashed*), CCA (*solid*) and Analogs (*dotted*)

Summarizing, several words about the potential benefits and limitations of the statistical methods should be said. Starting from the analog, it has been shown that the method demonstrates the worst performance in terms of standard deviation of the difference with KMH. At the same time, the data obtained with the analog method are not more biased than that from other statistical methods. This unbiased but too variable behavior can be partially explained by incompleteness of the analog pool, i.e., for this method, a fitting period longer than 5 years is required to accumulate the sufficient set of significant wave height patterns. This problem could be a strong limitation in case of applications to scenario studies, as wave situations that did not occur during the fitting period or were not included in the analog pool cannot be detected and reproduced by this method. The results of the CCA and LR are quite close to that from the KMH simulation with the LR demonstrating slightly more stable and accurate results. In addition, the LR provides the opportunity of the multiple downscaling, i.e. the simulation of several wave parameters simultaneously (for test examples see Gaslikova 2006). Although SWH represents one of the most frequently analyzed and most crucial wave parameter, other parameters are important for particular applications. For instance, from wave periods and wave heights, wave steepness can be inferred, which represents an important criterion in the design of ships and vessels. Another example that depends on wave period is the derivation of wave-induced bottom stress, which is important for the sediment transport and coastal erosion evaluations. Other parameters, such as wave direction, are crucial especially for extreme wave analysis within the coastal protection problem

where it is important to know from which direction the severe waves are coming.

Based on a balance between the quality of simulated data and required computational resources, LR appeared to be the most acceptable method for downscaling long-term wave data and obtaining small-scale wave statistics. It solves the problem of insufficient time and space resolution presented in multi-decade wave hindcasts and extremely high computational costs for long-term high resolution wave hindcasts. Considering all the comments, the linear regression is used for further multi-decade wave simulations in this study.

4 LOCAL WAVE CLIMATE FOR HELGOLAND

4.1 LOCAL EXTREME EVENTS

In this section the simulated wave climate for Helgoland is presented and discussed. The 3-hourly significant wave height fields for the Helgoland area were simulated with the linear regression model (as described in 3.1) for the period 1958-2001. The annual 75-th, 90-th and 99-th percentiles of the wave height distribution at each location were computed. To get an impression of the wave height spatial distribution dominating during past four decades, the means of these percentiles were derived and shown in Figure 8. In general, the SWH spatial distribution is characterized by the maximum wave heights in the western part of the model domain, gradual decrease of the wave heights further to the east and pronounced low wave area east to the islands.

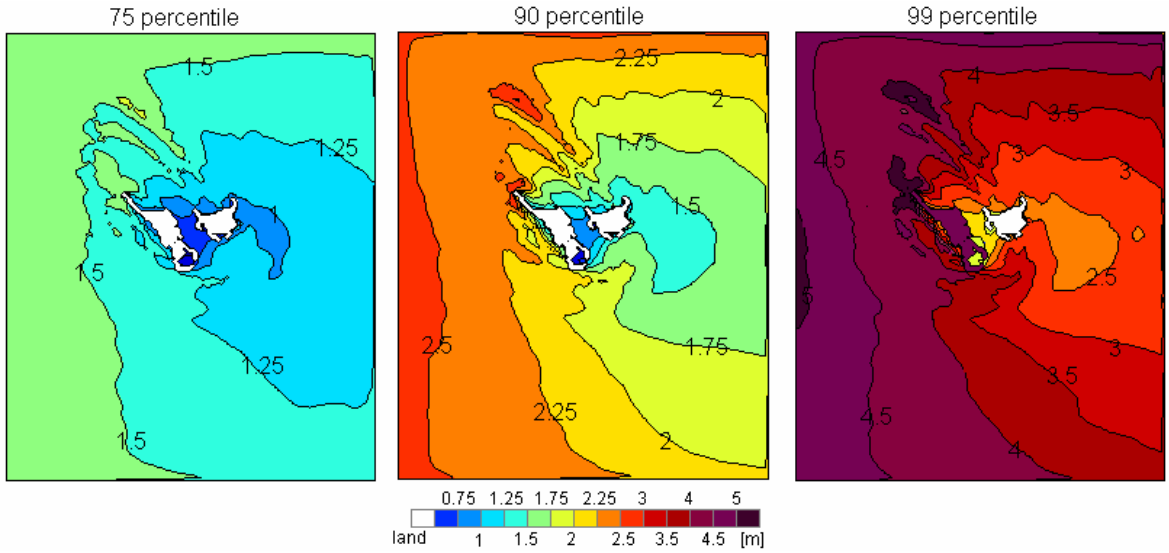

Fig. 8 Mean of the significant wave heights annual percentiles in meters for the period 1958-2001

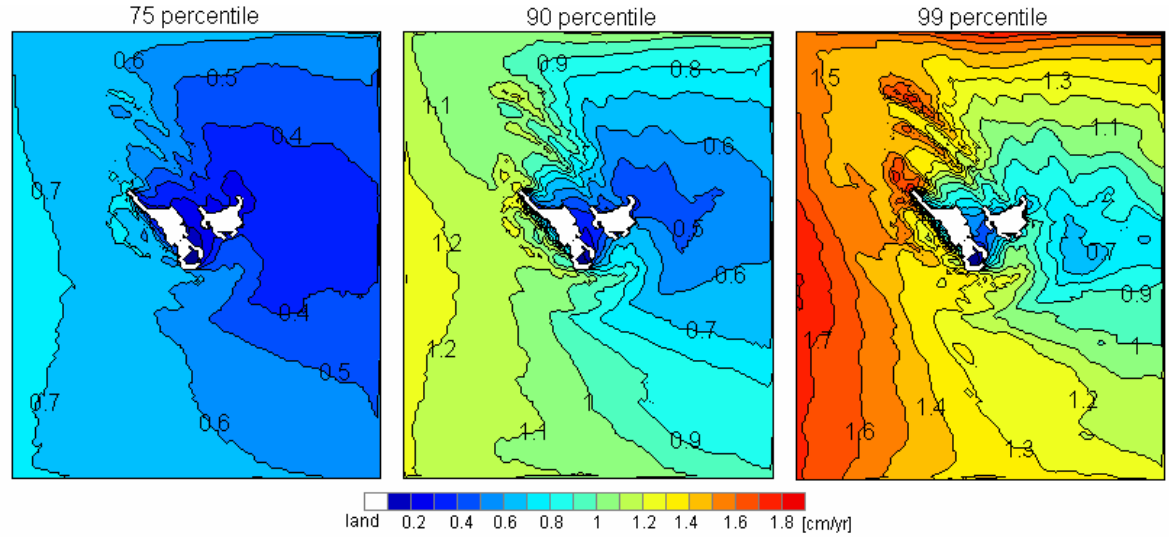

Fig.9 Trends for the annual percentiles of significant wave heights estimated for 1958-2001 period in cm/yr. The contour interval is 0.1 cm/yr

From the small-scale features the higher waves for the shoal north to the island and the higher waves directly to the south and south-east from the main island can be detected as well as constantly low wave region between the islands. This pattern is valid for all considered parts of SWH distribution and corresponds to the wave height spatial pattern associated with westerly wind conditions. This is consistent with the findings about the prevailing westerly wind conditions for the region (Gaslikova 2006). Most of the storm situations occur under the westerly winds, that explains the spatial patterns for the upper percentiles of wave height distribution.

Together with the mean wave statistics, the changes in wave climatology occurring during last decades are important. From the previous studies (e.g. WASA Group 1998) and the conclusions about the wind climatology the existence of the inter-annual trend for the SWH percentiles is hypothesized for the North Sea area and German Bight in particular. This hypothesis was tested on regional scale within the HIPOCAS project using the SWH data from HF hindcast. The significant positive trends of approximately 1.6 cm/year were detected for the 99-th percentiles of SWH in the vicinity of Helgoland (Weisse et al. 2003). The local linear trends for the selected three percentiles (75-th, 90-th and 99-th) of the wave height distribution at each location of the model domain are estimated and the results are presented in Figure 9. The significance of the obtained trends was tested with the two-sided T-test. It was found that the trends for 50-99 percentiles are significant with 1% error probability. The significance was detected for all locations of the model domain with the exception of the harbor area. Within the harbor the modeled wave heights do not show magnitudes higher than 1 m and are not affected by the intensification of the external wave extremes, which is the direct effect of the presence of the harbor with coastal protection constructions. On the other hand, the representation of the waves by the dynamical and statistical models within the harbor could not be completely adequate as the K-model and the linear regression method do not consider diffraction and were not designed for applications in such areas. In general, the areas of largest trends (Fig. 9) are correspondent to the areas where the highest waves were detected (Fig. 8), such as the western coast of the main island and the shoal north to the island. The magnitude of the maximum trends for the 99-th percentile (about 1.7 cm/yr) is in agreement with the HIPOCAS regional trends for the area (not shown). This is consistent with the nature of the LR hindcast obtained by downscaling of HF data. Any details and local tendencies, however, are available only from the high-resolution dataset.

4.2 EXTREME VALUES ANALYSIS

The information about the most severe wave conditions expected during the lifetime of the coastal constructions can be obtained from the wave height return values estimated from the known wave statistics. The SWH return value estimates were computed with the annual maxima method in which the Generalized Extreme Value Distribution (GEV) was fit to the sample of annual SWH maxima (e.g. Coles 2001). The LR SWH dataset for the period 1958-2001 was used for this analysis. For each location of the model domain and each year the SWH records were selected according to the corresponding wind directions and were grouped into eight SWH subsets according to the 45-degree wind direction sectors (similar as for LR model construction). The annual maxima at each group were then selected and the GEV distribution was fit for each location and each direction group based on the 44 SWH annual maxima. Finally, 20, 50 and 100-year return values were estimated from fitted distributions.

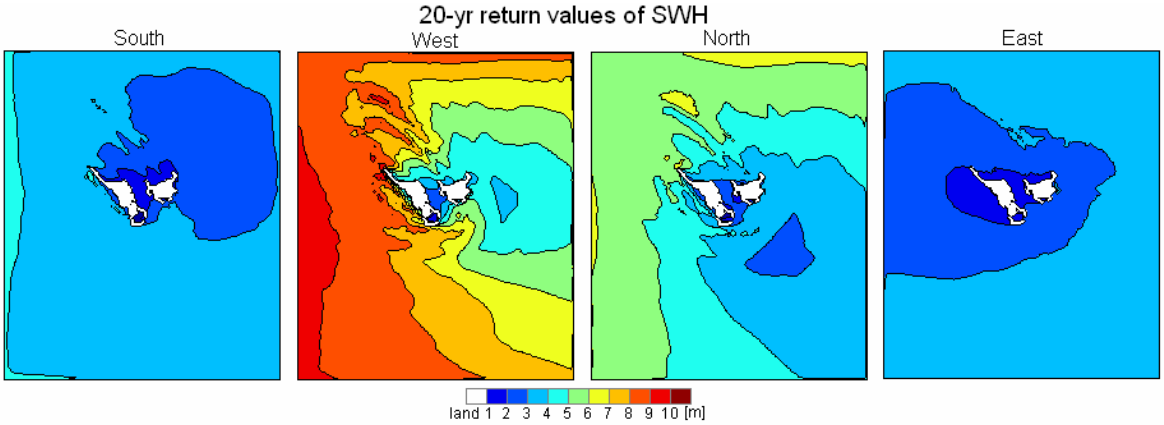

Fig.10 20-year return values of significant wave heights in meters estimated for the winds coming from southern, western, northern and eastern 45-degree sectors

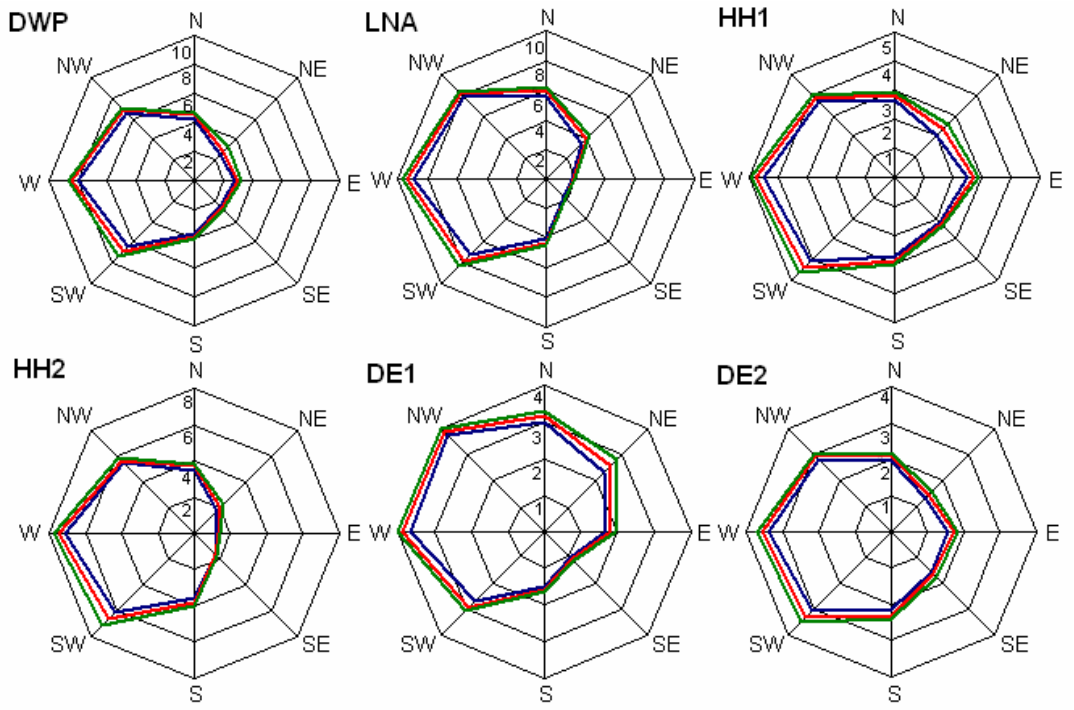

Fig.11 20 (*blue*), 50 (*red*) and 100 (*green*) year return values for significant wave heights in meters for selected locations and 8 wind direction sectors (winds are coming from). For the exact locations see Fig.1

In Figure 10 the examples of the SWH 20 year return values for four wind direction sectors are shown. Significant differences between the return values associated with different wind directions were revealed. While for easterly and southerly winds the 20-year return values appears to be not larger than 4 m, for westerly winds the estimated return values amount to 9 m magnitude. The spatial pattern of return values for westerly winds is close to that for the SWH 99-th percentiles (Fig. 8) demonstrating larger magnitudes than the SWH 99-th percentiles. This is consistent with the definition of the return value as an event happening once within a certain period (here 20 years) and the definition of the percentiles from which follows that for the LR wave data the events with wave heights equal or larger than annual 99-th percentiles occur during 30-40 time-steps (here 3-hourly intervals) a year.

The estimation of return values for different wind directions can be useful for engineering applications as soon as it defines the magnitude of the waves developed under certain wind conditions and the direction of their approach. As an example of the directional return value distribution, the 20, 50 and 100-year return values for the selected locations near Helgoland are shown in Figure 11. Some peculiarities related to the situation of the locations (see Fig.1) and revealed earlier in this work for the wave height extremes (4.1) can be detected for the return values as well. For LNA and DE1 the southeasterly winds produce minimum waves because of the island and breakwater presence; for the locations situated behind the island with respect to westerly winds, such as HH1, DE1, DE2, the return values are smaller than for the other locations. For each location the conditions and the approaching directions of the extreme events are detected. Similar information for any place of interest can be obtained with the GEV models.

5 CONCLUSIONS

Different approaches for obtaining high resolution near-shore wave statistics have been considered. A high-resolution dynamical wave simulation (KMH), based on an existing multi-decade wave hindcast for the North Sea, for the area around Helgoland for the period 1990–2001 was performed and found to reasonably represent observed wave conditions. Results of the KMH simulation were compared with the buoy and radar wave observations. The results demonstrated that the simulated wave data (SWH, peak period, and peak direction) generally show good agreement with measurements in terms of distributions, although upper percentiles of the modeled SWH appeared to be overestimated. The latter is partially caused by the boundary conditions that provide too high waves in case of severe storms.

The combination of dynamical and statistical approaches to the downscaling of medium-scale wave data was proposed as a faster alternative to the purely dynamical method. Three statistical models were built approximating the relation between instantaneous medium-scale and dynamically obtained local significant wave

heights. All three methods showed good skills in the representation of the wave height statistics, their results were comparable with the dynamically obtained results for long-term wave statistics and significantly improved the medium-scale data. That means most information about the local wave statistics was contained in the regional data and time-independent local features such as bathymetry, whereas the variable in time local fields such as currents or water level change played only a minor role in the formation of local wave statistics.

Although suffering from some uncertainties and limitations, the statistical-dynamical model has an irrefutable advantage of short computational time since the model is built for a certain area. The applicability of the described method to other coastal areas meets no principal objections, except that the considered area should have the connection to the open sea and, at least partially, be dependent on the regional wave climate. Of course, in each case the peculiarities of the area should be additionally considered and the most appropriate statistical model should be chosen.

Linear regression method, in combination with the dynamical wave model, allowed the production of a 44-year high-resolution wave hindcast for the Helgoland area, providing the wave statistics with the quality required by numerous coastal applications. Positive linear trends were revealed for annual extreme and mean wave heights on local scale, which corresponds with the results for regional wave data from earlier studies for the south-eastern North Sea. Although the general behaviour of annual wave extreme statistics was similar for the medium-scale and local data, the magnitude of the local wave extreme events as well as the rate of the inter-annual trends for high-resolution wave data differed significantly within the model domain, demonstrating the significance of local effects for the wave statistics. The assessment of the return values for the local wave heights was made based on the past wave statistics using the extreme values analysis. This method does not consider any inter-annual trends for the wave extreme events and, thereby, the nature and the direction of the trends are not important for this type of the analysis.

Statistical-dynamical approach is proposed as a tool for further assessments of future local wave climate and scenario studies. The low computational costs allow transferring necessary amount of regional scenarios to the local level. Thus, the results from different global and regional models as well as numerous scenarios can be considered. The range of local scenarios can be constructed providing more complete picture of potential local wave climate.

REFERENCES

Caires S, A Sterl, J-R Bidlot, N Graham, and V Swail, 2002: Climatological assessment of reanalysis ocean data. In *Proceedings of 7th international workshop on wave hindcasting and forecasting*, pages 1-12, Banff, Alberta, Canada

Cavaleri L and PM Rizzoli, 1981: Wind wave prediction in shallow water - theory and application. *J. Geophys. Res.*, 86:10961-10973

Coastal Engineering Manual, CHL, available at http://chl.erdc.usace.army.mil

Coles S, 2001: *An introduction to statistical modeling of extreme values*. Springer-Verlag, London

Cox AT and VR Swail, 2001: A global wave hindcast over the period 1958-1997: Validation and climate assessment. *J. Geophys. Res.*, 106(C2):2313-2329

Eurowaves project, available at http://www.oceanor.no/projects/eurowaves

Feser F, R Weisse, and H von Storch, 2001: Multi-decadal atmospheric modeling for europe yields multipurpose data. *EOS Transactions*, 82(28):305-310

Gaslikova L, 2006: *High-resolution wave climate analysis in the Helgoland area.* PhD thesis, Univ. of Hamburg

Günther H and Rosenthal W, 1995 A wave model with nonlinear dissipation source function. In *Proceedings of the 4th International workshop on wave hindcasting and forecasting*, Banff, Canada

Günther H, W Rosenthal, M Stawarz, JC Carretero, M Gomez, I Lozano, O Serrano, and M Reistad, 1998: The wave climate of the Northeast Atlantic over the period 1955-1994: the WASA wave hindcast. *Glob. Atmos. Ocean Sys.*, 6:121-163

Hasselmann K, TP Barnett, E Bouws, H Carlson, DE Cartwright, K Enke, JA Ewing, H Gienapp, DE Hasselmann, P Kruseman, A Meerburg, P Müller, DJ Olbers, K Richter, W Sell, and H Walden, 1973: Measurements of wind-wave growth and swell decay during the JOint North Sea WAve Project (JONSWAP). *D. Hydrogr. Z.*, A8(12):1-95

Hessner K, K Reichert, J Dittmer, JC Nieto Borge, and H Günther. Evaluation of WaMoS wave data. pp. 221-231, San Francisco

JERICHO project, available at http://www.satobsys.co.uk/Jericho

Kushnir Y, VJ Cardone, JG Greenwood, and MA Cane, 1997: The recent increase in North Atlantic wave heights. *J. Climate*, 10(8):2107-2113

Moghimi S, G Gayer, H Günther, and M Shafieefar, 2005: Application of 3-rd generation shallow water wave models in a tidal environment. *Ocean Dynamics*, 55(1):10-27

Schneggenburger C, H Günther, and W Rosenthal, 1997: Shallow water wave modelling with nonlinear dissipation. *Deutsche Hydrographische Zeitschrift*, 49:431-444

Schneggenburger C, 1998: *Spectral wave modelling with nonlinear dissipation*. PhD thesis, Univ. of Hamburg

Soares CG, R Weisse, JC Carretero, and E Alvarez, 2002: A 40 years hindcast of wind, sea level and waves in european waters. In *Proceedings of 21st International Conference on Offshore Mechanics and Arctic Engineering*

Sterl A, GJ Komen, and PD Cotton, 1998: Fifteen years of global wave hindcasts using winds from the European Centre for Medium-Range Weather Forecasts reanalysis: Validating the reanalyzed winds and assessing wave climate. *J. Geophys Res*, 103:5477-5492

von Storch H and FW Zwiers, 1999: *Statistical analysis in climate research*. Cambridge University Press

Vierfuss U, 2002: Ermittlung der Seegangsbelastung fur Helgoländer Molenbauwerke. *Hansa*, 139:68-73

WAMDI Group, 1998: The WAM model - a third generation ocean wave prediction model. *J. Phys. Oceanogr.*, 18:1775-1810

Wang XL and VR Swail, 2001: Changes of extreme wave heights in Nothern Hemisphere oceans and related atmospheric circulation regimes. *J. Climate*, 14:2204-2221

WASA Group, 1998: Changing waves and storms in the Northeast Atlantic? *Bull. Am. Meteorol. Soc.*, 79(5):741-760

Weisse R, F Feser, and H Günther, 2002: A 40-year high-resolution wind and wave hindcast for the Southern North Sea. pp. 97-104

Zorita E and H von Storch, 1999: The analog method as a simple statistical downscaling technique: comparison with more complicated methods. *J. Climate*, 12:2474-2489